Macromolecules

pubs.acs.org/Macromolecules Article

Tunable Interpenetrating Polymer Network Hydrogels Based on Dynamic Covalent Bonds and Metal−Ligand Bonds

Hui Yang, Sina Ghiassinejad, Evelyne van Ruymbeke,* and Charles-André Fustin*

Cite This: https://dx.doi.org/10.1021/acs.macromol.0c00494 Read Online

ACCESS | Metrics & More | Article Recommendations | Supporting Information

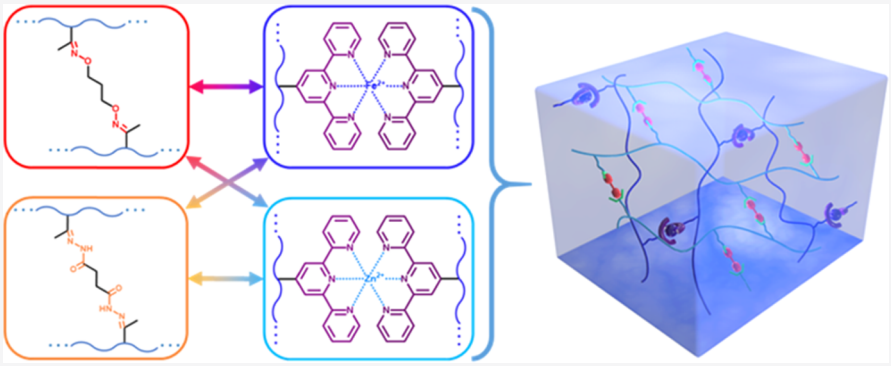

ABSTRACT: A series of tunable interpenetrating polymer network (IPN) hydrogels are designed by the orthogonal incorporation of two distinct types of reversible bonds, i.e., Schiff base bonds and metal−ligand coordination bonds. Two copolymers based on poly(*N*,*N*-dimethyl acrylamide) (PDMA) are synthesized and used as building blocks for the IPN hydrogels. The first one bears ketone pendant groups and is cross-linked by dihydrazide or bishydroxylamine compounds to form, respectively, hydrazine- or oxime-based dynamic covalent bond (DCB) networks. The second one bears terpyridine side groups and is cross-linked by the addition of two different transition-metal cations to obtain supramolecular networks based on metal−terpyridine bis-complexes. Several IPN hydrogels are prepared by combining these different types of reversible bonds to investigate how the two subnetworks influence each other. To this end, the influence of the cross-linker nature and of the hydrogel preparation protocol on the rheological properties of these IPNs are also studied in detail. In particular, we show that the obtained IPN hydrogels exhibit a higher modulus compared to the simple addition of the moduli of the single networks, which we attribute to the entanglements between the two networks. We then study how these IPN hydrogels can disentangle and partially relax if one of the reversible subnetworks is composed of cross-links with a shorter lifetime. Finally, pH is used as a stimulus to affect the dynamics of only one of the subnetworks, and the impact of this change on the properties of the IPNs is investigated.

■ INTRODUCTION

Polymer hydrogels, which are three-dimensional (3D) networks composed of cross-linked hydrophilic polymers entrapping substantial amounts of water,[1] are materials of choice for multiple applications such as drug delivery,[2] tissue engineering,[3] 3D printing,[4] wearable devices,[5] actuators,[6] energy-storage devices,[7] and bioelectronics.[8] To impart further tunability and adaptiveness to these hydrogels, dynamic or reversible cross-links are often used to build the networks.[9,10] These types of linkages encompass dynamic covalent bonds (DCBs) and supramolecular interactions, both of which can selectively and autonomously undergo reversible formation, breaking, and re-formation under equilibrium control.[11] In general, DCBs such as Schiff base bond (imine, acylhydrazone, and oxime), Diels−Alder adduct, disulfide bond, boronic ester bond, etc. have often relatively slow dynamics,[12] while supramolecular interactions including hydrogen bonding, metal−ligand complex, host−guest interaction, etc. have faster dynamics.[13] On account of the peculiar characteristics of DCBs and supramolecular interactions, the orthogonal combination of these two categories of cross-links to fabricate networks for responsive polymer hydrogels or elastomers has received a rapidly growing attention over the past few years.[14−20] Compared to networks based on a single type of cross-links, materials combining different cross-links possess desirable properties such as the ability to respond to multiple (orthogonal) stimuli, fast shape recovery, or good mechanical

Received: March 2, 2020
Revised: June 19, 2020

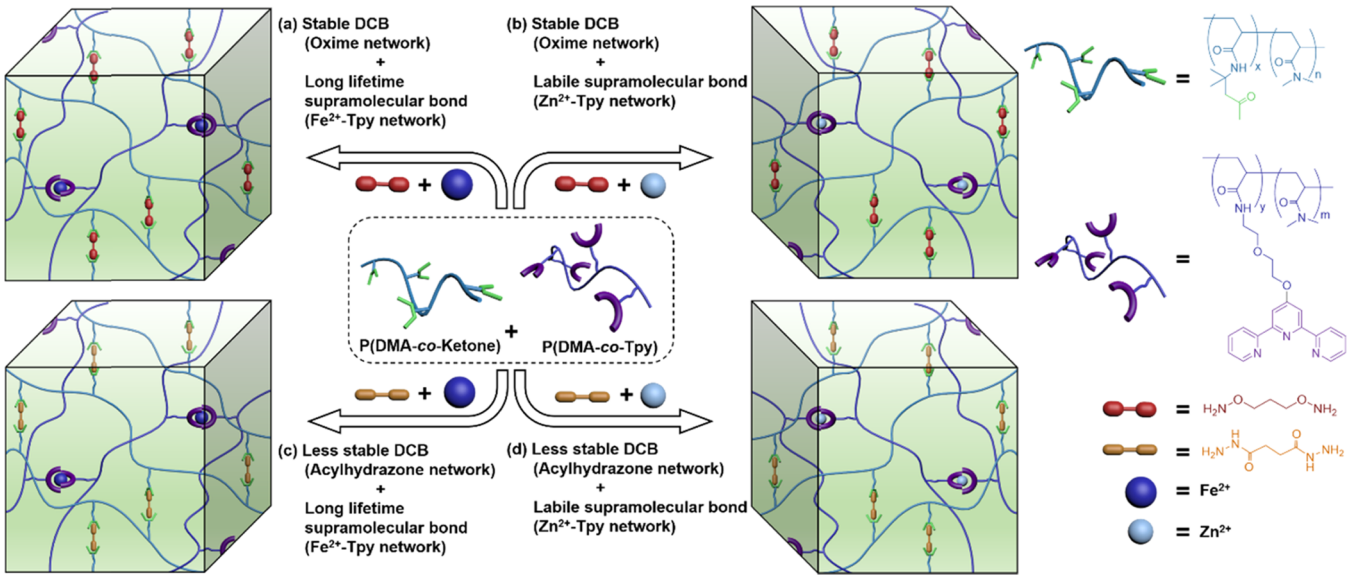

Figure 1. Schematic representation of four interpenetrating polymer network (IPN) hydrogels based on different combinations of dynamic covalent bond (DCB) (acylhydrazone or oxime bond) and supramolecular interaction (metal−terpyridine bis-complexes): (a) stable DCB and long-lifetime supramolecular bond (Oxime + Fe^{2+}−Tpy), (b) stable DCB with labile supramolecular bond (Oxime + Zn^{2+}−Tpy), (c) less stable DCB with long-lifetime supramolecular bond (Acylhydrazone + Fe^{2+}−Tpy), and (d) less stable DCB with labile supramolecular bond (Acylhydrazone + Zn^{2+}−Tpy).

properties such as high strength, toughness, and fatigue resistance.[17,20]

As a pH-sensitive bond formed by a "click" reaction[21] upon condensation between a carbonyl group and an amino derivative, Schiff base bonds are one of the most successful DCBs used so far in the preparation of responsive gels.[22−25] Interestingly, the hydrolytic stability of Schiff base bonds can be tuned in increasing order from imine, to acylhydrazone, to oxime by changing the primary amine to a hydrazide and to a hydroxylamine.[26] Due to their reversibility, and greater stability than imines, acylhydrazones and oximes have been used in the synthesis of functional gels in various fields.[24,27] Among supramolecular interactions, the metal−terpyridine coordination bond is the most attractive for the fabrication of responsive polymer gels since the bond characteristics (lifetime, strength) can be tuned over several orders of magnitudes simply by changing the metal ions used (or the ligand), it can be used in a range of solvents, and it may confer additional useful properties (catalytic, magnetic, photoactive, etc.) to the materials.[28−33] Therefore, in the present study, we investigate the rheological properties of polymer gels, which combine the aforementioned Schiff base bonds with metal−terpyridine coordination bonds, to create very stable—yet reversible—networks thanks to the presence of the DCBs, while keeping some room to tune the material properties, thanks to the metal−ligand interactions.

In general, several interactions can be combined by following either a "dual-network" approach or an "interpenetrating polymer networks" (IPNs) approach.[34] A dual network is generally made of the same polymer cross-linked by two different types of bonds, often a covalent and a supramolecular bond, or two types of supramolecular bonds,[20,35−37] while IPNs comprise two or more interlaced polymer networks that are not covalently bonded to each other. The latter systems have gained broad interest because they allow a combination of the desired properties of each network (e.g., stimuli responsiveness), and even more, because they may exhibit new properties that are not observed in the component networks alone.[38−44] Most notably, IPN hydrogels may show enhanced mechanical properties such as greater toughness, larger extensibility, and improved strength due to synergistic interactions between the component networks that transfer the stress and dissipate mechanical energy upon deformation.[34,45,46] Recently, the combination of DCB and supramolecular interactions has been also reported to fabricate responsive IPN hydrogels and elastomers with outstanding mechanical performances.[47−53] For example, Konkolewicz et al.[49] synthesized a double dynamic IPN elastomer with superior mechanical (increased stress and strain at break, increased malleability, greater toughness) and self-healing properties based on Diels−Alder adduct and hydrogen bonding. Liang et al.[52] prepared highly stretchable IPN hydrogels with the properties of actuation, shape memory, and self-healing capability using boronic ester bonds and alginate−Ca^{2+} complexation.

In this study, we investigate the viscoelastic properties of reversible IPN hydrogels formed through DCB and metal−ligand supramolecular interactions. In particular, we study how the rheological properties of both networks are combined and modified when these networks are interpenetrated. Since the DCBs (i.e., the acylhydrazone and oxime bonds) have been chosen to be very stable, we do not expect the samples to flow in the linear regime of deformation. However, the reversibility of the bonds could possibly be observed under large shear and/or in different environmental conditions (e.g., pH or temperature variation). On the other hand, depending on the metal ion selected, the lifetime of the supramolecular junctions can be easily varied. Therefore, the use of a supramolecular network made of labile interactions should allow us to study how the fast association/dissociation dynamics of the supramolecular network influences the overall response of the IPN hydrogels. Then, by exploiting metal−ligand interactions with long lifetime, we would like to see how the contribution of both the DCB and supramolecular networks can be

https://dx.doi.org/10.1021/acs.macromol.0c00494
Macromolecules XXXX, XXX, XXX−XXX

Table 1. Main Characteristics of P(DMA-*co*-ketone) and P(DMA-*co*-Tpy) Copolymers

copolymer	final ratio[a] (mol %)			M_n[b] (g/mol)	M_n[c] (g/mol)	Đ[c]	N_f/chain[d]	
	DMA	ketone	Tpy				ketone	Tpy
P(DMA-*co*-ketone)	96	4		40 000	56 000	1.32	16	
P(DMA-*co*-Tpy)	98.5		1.5	44 000	42 500	1.73		6

[a]Calculated from ^{1}H NMR spectra. [b]Evaluated by monomer conversion (^{1}H NMR). [c]Determined by SEC. [d]Average number of functional groups per chain.

distinguished. Finally, the cross-linking density or dynamics of the networks can be modified by varying the pH, which gives us an additional way to vary the relative stability of both networks.

To this end, we have synthesized a series of novel IPN hydrogels that are based on two functionalized hydrophilic copolymers (Figure 1). The first one bears ketone pendant groups and can be cross-linked by succinic dihydrazide or *O*,*O*′-(propane-1,3-diyl)bis(hydroxylamine) to form, respectively, acylhydrazone and oxime bonds, yielding Schiff base networks. The second copolymer bears terpyridine side groups and can be cross-linked by the addition of transition-metal cations (Zn^{2+} and Fe^{2+} were used in this work) to form metal−terpyridine bis-complexes. Therefore, the obtained interpenetrated networks are composed of a DCB-cross-linked network and of a supramolecularly cross-linked network. Thanks to the different nature of the cross-linkers, the bond strength and kinetic stability of the DCB (acylhydrazone or oxime) and supramolecular interaction (Fe^{2+}−terpyridine or Zn^{2+}−terpyridine bis-complexes) can be independently tuned. As shown in Figure 1, four IPN hydrogels have thus been obtained by combining these interactions in different ways. First, a very stable (i.e., characterized by a high equilibrium constant) DCB is combined with a long-lifetime supramolecular interaction (Oxime + Fe^{2+}−Tpy) or with a more dynamic supramolecular interaction (Oxime + Zn^{2+}−Tpy). Second, a less stable DCB is combined with the long-lifetime supramolecular interaction (Acylhydrazone + Fe^{2+}−Tpy) or with the more dynamic supramolecular interaction (Acylhydrazone + Zn^{2+}−Tpy). The influence of these different combinations of interactions on the IPN properties is investigated in detail by rheology.

■ RESULTS AND DISCUSSION

Synthesis of Hydrophilic-Functionalized Copolymers. We have chosen the hydrophilic biocompatible poly(*N*,*N*-dimethyl acrylamide) (PDMA) as the backbone polymer for fabricating the hydrogels. The commercially available comonomer, diacetone acrylamide (DAAM), which contains a ketone group that can react with dihydrazide or bishydroxylamine compounds to form acylhydrazone or oxime bonds, was employed to create Schiff base bond-based networks (Figure 1). The hydrophilic terpyridine-functionalized monomer (*N*-(2-(2-([2,2′:6,2″-terpyridine]-4′-yloxy)ethoxy)ethyl)-acrylamide (TPy-DEG-AM)) was synthesized in two steps from commercially available precursors (see the Supporting Information) and can form metal−terpyridine bis-complexes with various strengths and labilities in combination with transition-metal ions. The copolymers that will be the precursors of the network were prepared by copolymerizing functionalized monomers, i.e., one bearing a ketone group and the other bearing a terpyridine, with the base monomer of DMA. Reversible addition−fragmentation chain transfer (RAFT)-controlled radical polymerization was used to this aim. Two copolymers, P(DMA-*co*-ketone) and P(DMA-*co*-Tpy), were obtained in this way and were characterized by NMR and size-exclusion chromatography (SEC) (Table 1).

Preparation of Networks. The P(DMA-*co*-ketone) copolymer was used as a precursor for preparing acylhydrazone/oxime networks, and the P(DMA-*co*-Tpy) copolymer was used for the formation of metal−ligand networks. For all of the prepared networks, the amount of added cross-linkers (dihydrazides, bishydroxylamines, or transition-metal cations) was half an equivalent compared to the reaction sites (ketone groups or terpyridine groups) of the copolymers. Three types of networks of increasing complexity were prepared to allow the systematic comparison of their rheological properties and the determination of the respective contributions of the two types of bonds. Individual networks were prepared from each of the above copolymers with corresponding cross-linkers (Schemes S5 and S6). Single networks were prepared from mixed solutions of the two copolymers but cross-linking only one of the copolymers with the appropriate cross-linker (Scheme S7). Interpenetrating polymer networks were prepared also from mixed solutions of the two copolymers, but this time cross-linking both copolymers (Scheme S8).

Formation of individual networks from each of the two above copolymers has been first investigated in deionized water (pH: 6−7). We found that the P(DMA-*co*-ketone) copolymer reacts with the dihydrazide cross-linker to form acylhydrazone hydrogels after 1 day, and with bishydroxylamine cross-linker to form oxime hydrogels after 9 h at a copolymer concentration of 10 wt %. At lower concentrations, P(DMA-*co*-ketone) cannot form gels with these cross-linkers even after 1 month of reaction. The P(DMA-*co*-Tpy) copolymer is cross-linked by Fe^{2+} ions in a few minutes via the formation of Fe^{2+}−terpyridine bis-complexes (Fe^{2+}−Tpy) at a minimum copolymer concentration of 6 wt %. Therefore, concentrations of 10 wt % for the P(DMA-*co*-ketone) copolymer and of 6 wt % for the P(DMA-*co*-Tpy) copolymer have been adopted in this work for network preparation. In addition, two single networks were also prepared at a total polymer concentration of 16 wt % by mixing both copolymers together, 10% of P(DMA-*co*-ketone), and 6% of P(DMA-*co*-Tpy), but inducing the cross-linking of only one of the copolymers with the appropriate reagent.

The IPN hydrogels were prepared by adding dihydrazide or bishydroxylamine and metal ions (Zn^{2+} or Fe^{2+}) to solutions of mixed copolymers: 10 wt % P(DMA-*co*-ketone) and 6 wt % P(DMA-*co*-Tpy) to reach a total polymer concentration of 16 wt % as for the single networks. The influence of the addition sequence of cross-linkers, i.e., inducing first the DCB formation and then the metal−ligand bonds or the reverse, on the rheological properties of the obtained IPNs was studied. In each case, a 24 h waiting time was applied before adding the second cross-linker.

Rheological Characterization. Oscillatory shear rheology was used as the main characterization method to investigate

https://dx.doi.org/10.1021/acs.macromol.0c00494
Macromolecules XXXX, XXX, XXX−XXX

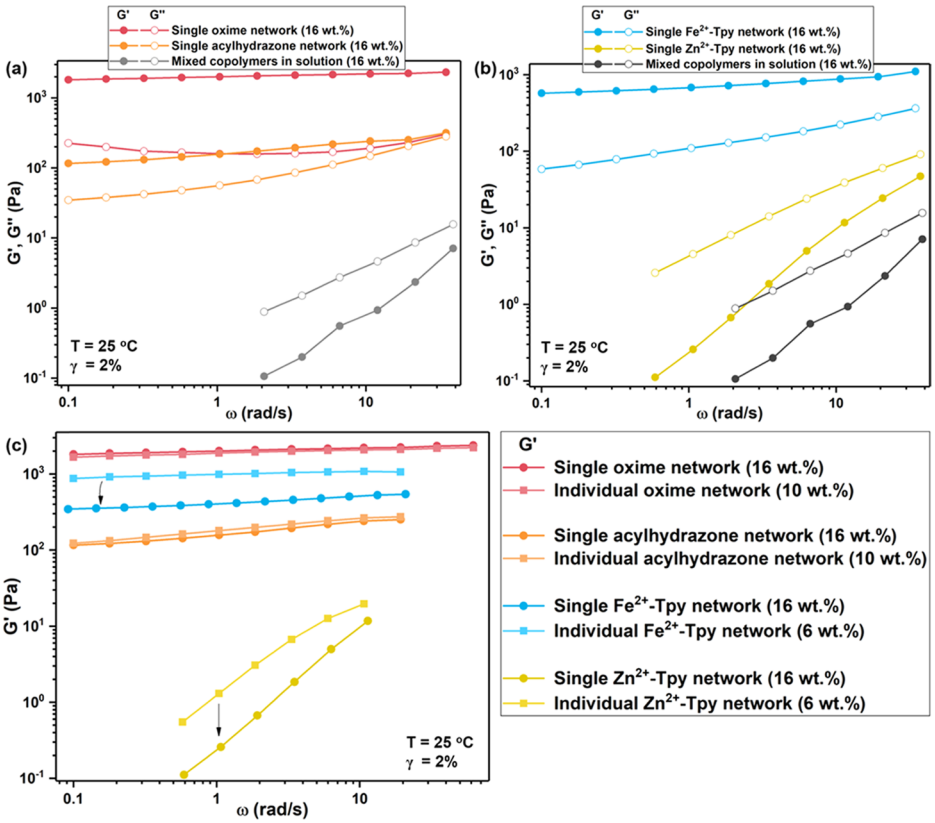

Figure 2. Oscillatory frequency sweeps on single networks based on (a) acylhydrazone and oxime and (b) on Fe^{2+}−Tpy and Zn^{2+}−Tpy from the mixed copolymer solution of P(DMA-*co*-ketone) and P(DMA-*co*-Tpy). (c) Comparison of the storage modulus of individual and single networks of oxime, acylhydrazone, Fe^{2+}−Tpy, and Zn^{2+}−Tpy.

the dynamic mechanical properties of all networks under shear. The dynamic covalent bonds generally exhibit higher bond dissociation energies and slower dynamics than supramolecular interactions.[12,17] In our case, the order of rate constants for the formation of cross-links between two chains is approximately acylhydrazone < oxime < Zn^{2+}−Tpy < Fe^{2+}−Tpy at 25 °C in water (pH ∼ 7).[54−58] Therefore, we first measured the oscillatory shear rheological behavior of the individual acylhydrazone hydrogel, i.e., the slowest-forming network according to the above data, at different aging times to determine the best preparation time to achieve stable and reproducible frequency sweeps. Amplitude sweep measurements were also performed to determine the limit of the linear regime of deformation. As depicted in Figure S3, the rheological behavior of individual acylhydrazone hydrogels did not change significantly after 2 days of aging, indicating that a stable state has been reached. Based on these results, all of the following rheology measurements on all hydrogels have been executed after 2 days of aging time at room temperature.

The dynamic viscoelastic behaviors of individual networks of oxime, acylhydrazone, Fe^{2+}−Tpy, and Zn^{2+}−Tpy were measured by oscillatory frequency sweeps (Figure S4). For these four samples, the storage moduli (G') are always higher than their pure copolymer solutions, indicating the formation of cross-links after 2 days of aging. ^{1}H NMR characterizations (Figure S5) also proved the formation of oxime and acylhydrazone cross-links. The storage moduli of the acylhydrazone, oxime, and Fe^{2+}−Tpy samples are almost constant over the whole experimental frequency window, showing that stable gels have been formed. Their values, which are close to 1 kPa for oxime and Fe^{2+}−Tpy, and close to 200 Pa for acylhydrazone, can be compared to the values found if we assume that all of the functional groups lead to the creation of effective intermolecular cross-links, i.e., $G_N^0 = \frac{c\rho_0 RT}{M_{XX}}(1 - \varphi_{dangling})$, where ρ_0 is the density of PDMA in the melt state (approximated as 1 g/cm^3), c is the sample concentration, M_{XX} is the average molar mass between two sticky groups (estimated to be 2.5 kg/mol for P(DMA-*co*-ketone) and 7.3 kg/mol for P(DMA-*co*-Tpy); see Table 1), and $\varphi_{dangling}$ is the weight fraction of dangling ends, which do not participate in the network elasticity and can be approximated as equal to $2M_{XX}/M_w$. In such a case, the plateau moduli of the P(DMA-*co*-ketone) and the P(DMA-*co*-Tpy) samples should be approximately equal to 89 and 16 kPa, respectively, which are much higher than the values found experimentally. This result suggests the presence of a large number of unreacted groups, as well as the presence of internal loops due to intramolecular cross-links that do not contribute to the sample elasticity, especially in the case of the acylhydrazone network. The higher level of the plateau modulus of the oxime network is due to a higher cross-linking density of oxime hydrogels, consistent with the greater equilibrium constant and the greater intrinsic hydrolytic stability of oximes compared to acylhydrazones.[58]

On the other hand, the relatively higher level of the rubbery plateau observed for the Fe^{2+}−Tpy system (compared to the value found in the case of the perfect network) demonstrates its larger capability to create intermolecular junctions. This can be due to both the high association constant of Fe^{2+}−terpyridine bis-complexes[54] and the fact that the molecular

https://dx.doi.org/10.1021/acs.macromol.0c00494
Macromolecules XXXX, XXX, XXX−XXX

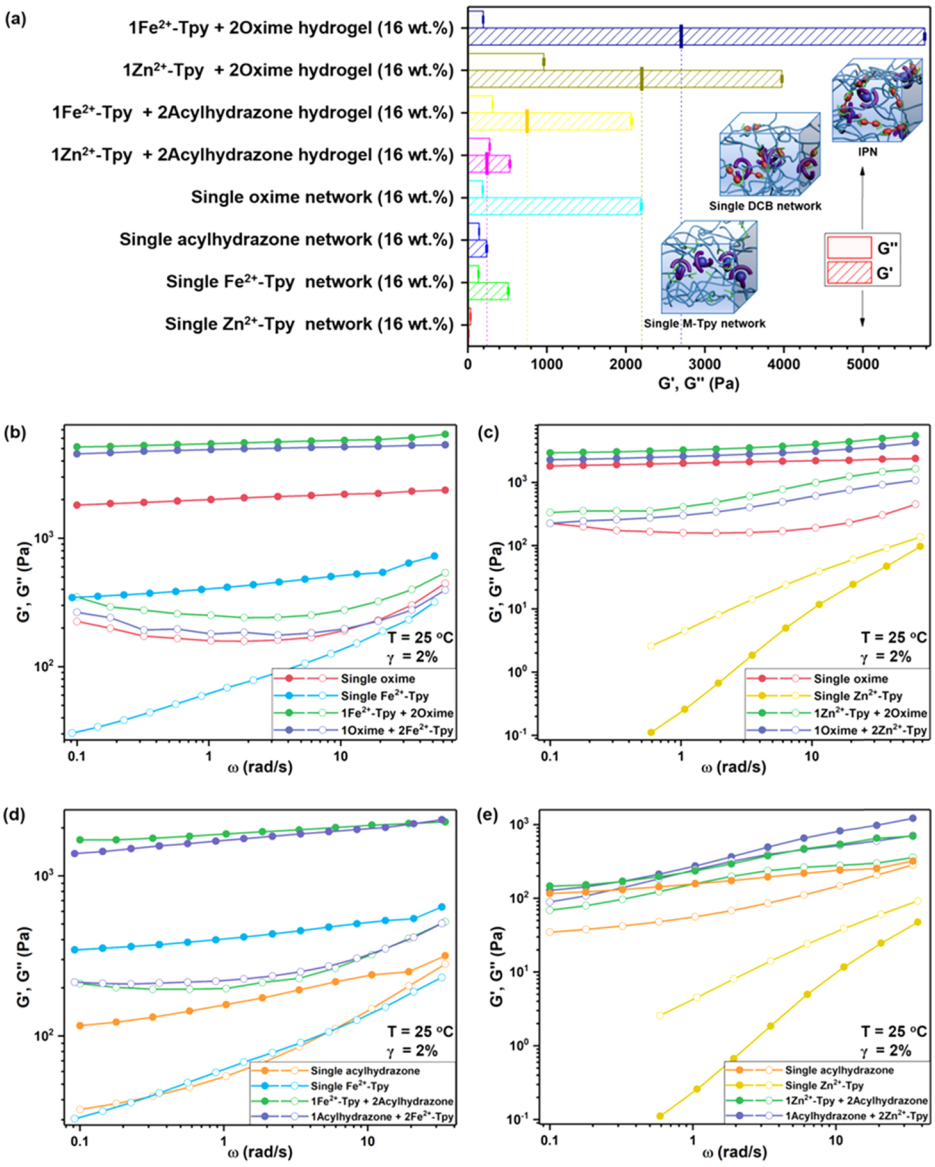

Figure 3. (a) Summary of the dynamic moduli values for the different IPN hydrogels and the corresponding single networks. The values were obtained from the frequency sweeps at a frequency of 10 rad/s. The vertical lines on the G' bar of the four IPN hydrogels represent the sum of the G' of the corresponding single networks. (b−e) Oscillatory frequency sweeps on the IPN hydrogels and their corresponding single networks (G': filled symbols, G'': open symbols). The numbers 1 and 2 in the sample names refer to the addition sequence of the cross-linkers.

strands between two sticky groups are longer, which reduces the probability of creating internal loops. Only the system based on Zn^{2+}−Tpy associations is able to flow within the experimental frequency window. This is attributed to the lower equilibrium constant and high lability of Zn^{2+}−terpyridine bis-complexes,[54] which largely reduce the lifetime of the supramolecular network.[28] Moreover, at a high frequency, a power law of 1/2 is found for $G'(\omega)$, indicating that before the terminal regime, the relaxation of this material is well described by a (constraint release) Rouse process.

Next, the possible influence of free chains (non-cross-linked) of the other copolymer type on the network properties is investigated, as shown in Figure 2a,b. These single networks contain 10 wt % P(DMA-*co*-ketone) and 6 wt % P(DMA-*co*-Tpy) and only one type of cross-linker. Figure 2c compares their storage moduli to the ones of their individual networks. It is seen that the viscoelastic response of the acylhydrazone and oxime samples is not influenced by the presence of P(DMA-*co*-Tpy) chains, which suggests that there is no interaction between P(DMA-*co*-ketone) and P(DMA-*co*-Tpy) chains when the P(DMA-*co*-ketone) copolymer is cross-linked in the presence of the other copolymer type. This also highlights the fact that the unassociated chains (or dangling ends) are relaxing very fast compared to the lifetime of the associated dynamic covalent interactions and do not contribute to the sample elasticity in the frequency window measured experimentally.

In the case of the supramolecular networks (Fe^{2+}−Tpy and Zn^{2+}−Tpy), the comparison between the dynamic mechanical properties of their single and individual supramolecular networks shows that mixing the two copolymers slightly reduces the level of the elastic modulus. The reason behind this could be a "screening effect" induced by the presence of a large amount of the nonactive P(DMA-*co*-ketone) copolymer compared to the P(DMA-*co*-Tpy) copolymer (10 vs 6%), slightly reducing the proportion of associated stickers or

https://dx.doi.org/10.1021/acs.macromol.0c00494
Macromolecules XXXX, XXX, XXX−XXX

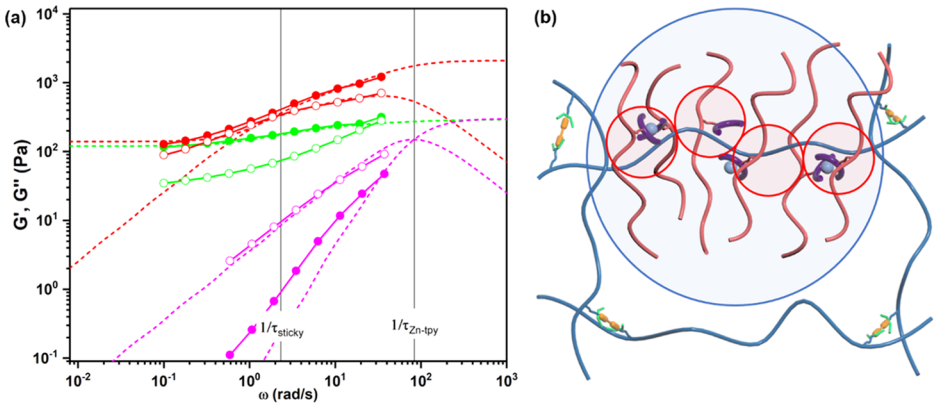

Figure 4. (a) Experimental (symbols) and theoretical (dashed curves) storage (full symbols) and loss moduli (empty symbols) of the single Zn^{2+}−Tpy network (magenta), the single acylhydrazone network (green), and the 1Acylhydrazone + 2Zn^{2+}−Tpy IPN (red). (b) Cartoon representing the sticky Rouse relaxation of the molecular segments in the acylhydrazone network (represented in blue). While at very short times, interactions with the Zn^{2+}−Tpy network (in red) prevent the motion of these segments (see the red blobs), at longer times, the segments are able to explore a larger surrounding (see the blue blob) and partially relax, at the rhythm of dissociations−associations of the Zn^{2+}−Tpy network.

promoting the formation of internal loops and therefore affecting the, already low, cross-linking density of Fe^{2+}−Tpy and Zn^{2+}−Tpy.

Knowing the dynamics of the single networks, we can now investigate the viscoelastic properties of the four IPN hydrogels, which are presented in Figure 3. There are several points to highlight here. First, as for the single networks, the frequency dependence of the storage modulus of most of the IPNs is very limited, showing only a weak decrease with decreasing frequency, indicating that stable gels have been formed. As expected, the storage modulus measured at 10 rad/s, $G'(\omega = 10$ rad/s), is larger for the IPN containing the more stable bonds, i.e., 1Fe^{2+}−Tpy + 2Oxime, with $G'(\omega = 10$ rad/s) = 5780 Pa. The modulus then takes lower value for the IPNs 1Zn^{2+}−Tpy + 2Oxime (3975 Pa) and 1Fe^{2+}−Tpy + 2Acylhydrazone (2072 Pa) and becomes very small for the IPN 1Zn^{2+}−Tpy + 2Acylhydrazone (532 Pa). The latter value is not representative of the plateau modulus since it is taken in the flow regime of the sample. Furthermore, it is observed that the addition order of the two cross-linkers has a slight influence on the dynamic mechanical properties of the IPNs. For the systems with at least one long lifetime cross-link type, i.e., Fe^{2+}−Tpy + Oxime, Zn^{2+}−Tpy + Oxime, and Fe^{2+}−Tpy + Acylhydrazone (Figure 3b−d), adding first the metal ions (Zn^{2+}, Fe^{2+}) to build the supramolecular network, followed by the addition of dihydrazide/bishydroxylamine to create the second network yields IPNs with slightly higher moduli. This could come from the greater chain mobility of the P(DMA-*co*-ketone) copolymer inside the more sparsely cross-linked supramolecular first network, compared to the reverse cross-linking order where the denser DCB network is formed first, allowing a slightly easier and more efficient formation of the second network. On the other hand, the less stable DCB with labile metal−ligand bond (Acylhydrazone + Zn^{2+}−Tpy) system shows the opposite behavior, the dynamic moduli of the IPN being higher when the acylhydrazone cross-links are formed before the Zn^{2+}−Tpy cross-links (Figure 3e). This could be explained by the fact that the viscoelastic response of the IPN in which Zn^{2+}−Tpy cross-links are formed first does not easily reach its equilibrium state, as confirmed by Figure S6, which shows that the moduli of this IPN reach the same level as for the other one after 1 month of aging.

An interesting point to observe in Figure 3 is the fact that the storage modulus of each IPN hydrogel is higher than the sum of their single network hydrogels. For example, the sum of the storage modulus of the single Fe^{2+}−Tpy hydrogel (511 Pa) and oxime hydrogel (2194 Pa) is only equal to 2705 Pa, which is much lower than that of the corresponding IPN hydrogel (5780 Pa). These results indicate a synergetic behavior between the two interpenetrating networks which stiffens the IPN hydrogels beyond the simple sum of the moduli (Figure 3a). This enhanced modulus of IPN hydrogels most probably arises from the fact that part of the entanglements created between the P(DMA-*co*-ketone) and P(DMA-*co*-Tpy) chains due to the two cross-linked networks can now be trapped between associated stickers, and therefore act as additional physical interactions governed by the dynamics of the stickers. Thus, the IPN elasticity is not only due to the associated reversible junctions but also due to the possible interactions between the chains.

While the influence of blending two networks on the sample elasticity is clearly observed in Figure 3a, it is also important to investigate how it influences the relaxation dynamics of the IPN. To this end, we focus on the IPN containing Zn^{2+}−Tpy junctions since the relaxation of the complexes is fast enough to be measured under the conditions used here. The Zn^{2+}−Tpy + Acylhydrazone IPN shows the strongest frequency dependence since it is made of the two weakest bonds (Figure 3e). The decrease of G' with frequency for this IPN is proportionally more pronounced than for the acylhydrazone single network, showing that this decrease is mainly due to the relaxation of the Zn^{2+}−Tpy network, which allows in turn the release of both the supramolecular network elasticity and the interactions between the two networks. As shown in Figure 4, we also observe that the relaxation of the Zn^{2+}−Tpy network within this IPN starts at a time similar to the relaxation time of the single Zn^{2+}−Tpy network. However, a much longer time is required before the contribution of the Zn^{2+}−Tpy network fully vanishes and the IPN reaches the modulus of the acylhydrazone single network. In the transition zone between these two times, a characteristic slope of −1/2 is observed in the storage modulus, indicating a Rouse relaxation. This result can be understood as follows: the IPN elasticity mostly arises from the interactions between the two networks. With time, since the Zn^{2+}−Tpy complexes of the supramolecular network

https://dx.doi.org/10.1021/acs.macromol.0c00494
Macromolecules XXXX, XXX, XXX−XXX

continuously dissociate and associate, the molecular segments located between two DCBs of the acylhydrazone network are able to explore their surrounding, but only at the rhythm of the relaxation (or association/dissociation dynamics) of the supramolecular bonds (see Figure 4b). Therefore, this slow (and partial) relaxation of the acylhydrazone network segments is well described by a sticky Rouse process[59,60]

$$G(t) = G_N^0\phi(t) + G_N^0 \sum_{p=1}^{N_{Zn-Tpy}} \exp\left(\frac{-p^2 t}{\tau_{Zn-Tpy} N_{Zn-Tpy}^2}\right) \quad (1)$$

where G_N^0 is the plateau modulus of the acylhydrazone network, $\phi(t)$ is the fraction of the acylhydrazone network which is not relaxed at time t, N_{Zn-Tpy} is the number of interactions between the acylhydrazone and Zn^{2+}−Tpy networks located between two associated DCBs, and τ_{Zn-Tpy} is the average lifetime of the Zn^{2+}−Tpy network. This model is tested in Figure 4a, in which we consider that $\tau_{Zn-Tpy} = 0.012$ s (as determined by approximating the viscoelastic response of the single network by a single Maxwell mode), $G_N^0 = 300$ Pa (as observed experimentally), and considering a stretched exponential function to approximate the relaxation function $\phi(t)$ of the single acylhydrazone network (green curve), $\phi(t) = 0.5 + 0.5\exp(-t^{0.5})/0.45$.

The only unknown parameter is the number of network−network interactions per segment of the acylhydrazone network, which determines both the level of the high-frequency rubbery plateau of the IPN and the time needed for the influence of the Zn^{2+}−Tpy network to disappear. This number must be fixed to 6 to correctly describe the experimental data (Figure 4a).

These results suggest that the partial relaxation of the long-lifetime network takes place through sticky Rouse relaxation process. This means that the time needed to recover the same elasticity as in the single, long-lifetime network, τ_{sticky}, is N_{Zn-Tpy}^2 times longer than the lifetime of the short-lifetime network.

A short comment should be made here. Usually, sticky Rouse relaxation is observed with dual networks[61] and not with interpenetrated networks. To be exact, one could argue that the Rouse regime observed in Figure 4a is not a sticky Rouse process, but rather a constraint release Rouse regime, where the molecular segments of the acylhydrazone network partially relax thanks to the disentanglement and relaxation of the Zn^{2+}−Tpy network, as described in ref 62. However, since the relaxation of the Zn^{2+}−Tpy network is fully governed by the relaxation of the supramolecular complexes, it seems appropriate to define this Rouse regime by a sticky Rouse relaxation.

The viscoelastic response of the 1Oxime + $2Zn^{2+}$−Tpy IPN can also be modeled based on eq 1 (Figure 5). In this case, we consider the same relaxation time τ_{Zn-Tpy} as with the 1Acylhydrazone + $2Zn^{2+}$−Tpy IPN since the oxime network is diluted in the same short-lifetime network. Furthermore, the plateau modulus of the single oxime network is fixed from the experimental data as equal to 2100 Pa, while the function $\phi(t)$ is well approximated by $\phi(t) = 1$. The number of interactions per molecular segment between the two networks is, again, determined by best fitting. We find that ($N_{Zn-Tpy} = 2$) leads to a good agreement between the theoretical and the experimental data (Figure 5). This lower value is a direct consequence of the fact that the oxime network is much denser than the acylhydrazone network. Therefore, the molecular segments between two associated DCBs are shorter, which limits the number of interactions with the Zn^{2+}−Tpy network.

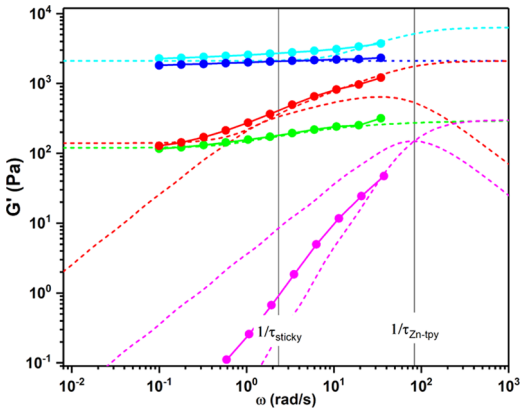

Figure 5. Experimental (symbols) and theoretical (dashed curves) storage modulus of the single Zn^{2+}−Tpy network (magenta), the single acylhydrazone network (green), 1Acylhydrazone + $2Zn^{2+}$−Tpy IPN (red), single oxime network (blue), and 1Oxime + $2Zn^{2+}$−Tpy IPN (cyan).

When Fe^{2+} ions are used instead of Zn^{2+} in the supramolecular network, the lifetime of the complexes becomes too long to easily observe its relaxation. As shown in Figure S7, the loss modulus of the single Fe^{2+}−Tpy network only starts to increase at a frequency of around 0.01 rad/s, which indicates the beginning of the network relaxation. Nevertheless, the data suggest that, similarly to the 1Acylhydrazone + $2Zn^{2+}$−Tpy IPN, partial relaxation of the 1Acylhydrazone + $2Fe^{2+}$−Tpy IPN starts to take place at a time equal to the lifetime of the complexes, followed by a Rouse-like relaxation. This behavior is thus similar to the one with the Zn^{2+}−Tpy complexes, but it is slowed down by around 3 orders of magnitude.

To speed up the partial relaxation of these IPNs, external conditions must be changed. In the following, we investigate the influence of a reduced pH on the dynamics of the IPN hydrogels. Indeed, as mentioned in the Introduction section, due to the fact that Schiff base bonds are pH-sensitive[58] and that the protonation of the terpyridine ligand weaken the metal−terpyridine coordination bonds,[63] the IPN hydrogels are expected to have the ability of gel−sol transition by changing the pH of the environment. To study the pH responsiveness of the prepared IPN hydrogels, HCl (2 M) and triethyl-amine were used as pH regulators. As mentioned above, all IPN hydrogels were prepared from pure water at pH 6−7.

Figure 6 presents the rheology data on the four IPNs at different pH values. Most IPN hydrogels stay in the gel state even at low pH (Figure 6a−c), apart from the Acylhydrazone + Zn^{2+}−Tpy IPN, made of the two weakest bonds, which turns into a solution at pH 1−2, showing that both subnetworks have been fully destructured (Figure 6d). The oxime-based IPN hydrogels (Figure 6a,b) and the corresponding individual oxime network (Figure S8a) are least affected by the pH change. This difference compared to the acylhydrazone-based systems (Figure 6c,d) can be attributed to the higher resistance toward hydrolysis of oxime compared to acylhydrazone bonds.[26,58,64]

We also observe that the individual network based on Fe^{2+}−Tpy complexes (Figure S9a) is more affected by pH than the individual oxime network (Figure S8a), as can be seen by the

https://dx.doi.org/10.1021/acs.macromol.0c00494
Macromolecules XXXX, XXX, XXX−XXX

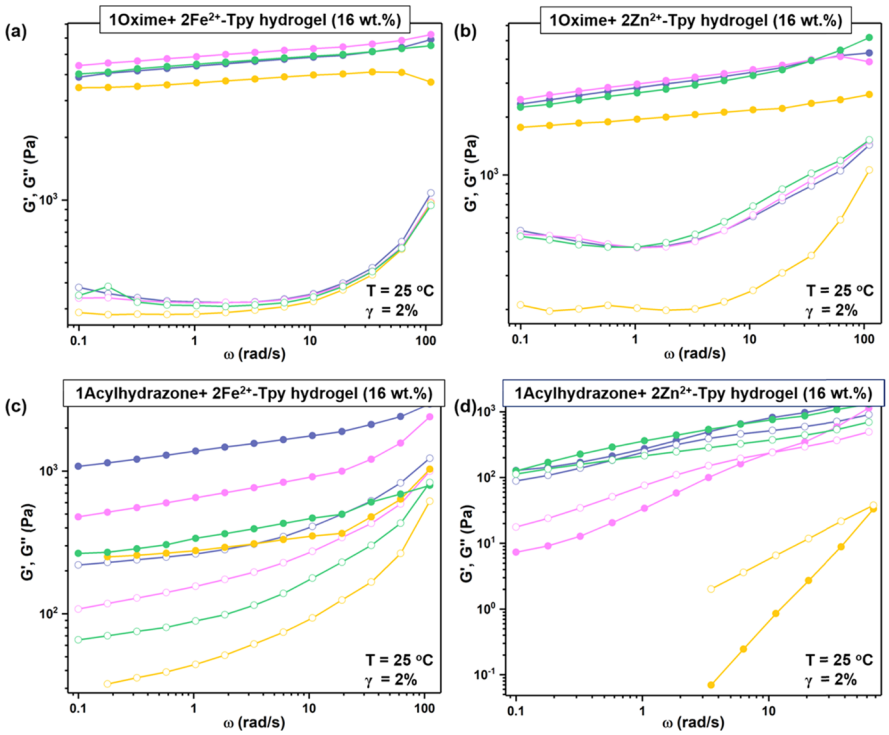

Figure 6. pH dependence of the dynamic moduli (G': filled symbols, G'': empty symbols) of the IPN hydrogels. Blue curves: initial hydrogel at pH 6−7, pink curves: pH 3−4, yellow curves: pH 1−2, green curves: back to pH 6−7.

drop of modulus by a factor of around 2.5 at pH 1−2, indicating that a lower number of complexes are formed at this pH. However, even at pH 1−2, this sample still displays a second, low-frequency plateau, which can be attributed to the long relaxation time of the supramolecular complexes. The influence of pH is much more important for the 1Acylhydrazone + 2Fe^{2+}−Tpy IPN since low pH completely fluidizes the acylhydrazone individual network (Figure S8b). Therefore, at low pH, the contribution of acylhydrazone to the IPN is only observed at a high frequency and vanishes at longer time, at which the IPN behaves similarly to the individual Fe^{2+}−Tpy network, i.e., as if the acylhydrazone network was not present. Playing with the pH is thus a way to promote the reversible dynamics of this IPN, otherwise too stable at neutral pH. In particular, at low pH, it is the DCB network that is relaxing first, not the Fe^{2+}−Tpy supramolecular network as it is the case at neutral pH (see Figure S7).

For the two other IPNs (Figure 6b,d), the association dynamics of the Zn^{2+}−Tpy network is always much faster than that of both DCB networks. Therefore, at a low frequency, the G' and G'' moduli of the Acylhydrazone + Zn^{2+}−Tpy and Oxime + Zn^{2+}−Tpy IPNs are similar to the ones of the DCB individual network, showing that the Zn^{2+}−Tpy network is completely destructured and only the acylhydrazone and oxime networks partially remain (Figure S8).

From Figure 6, we also note that three out of the four IPN hydrogels show complete recovery when the pH is returned to its original value. Only the Acylhydrazone + Fe^{2+}−Tpy IPN cannot recover its original state. This may be explained by the fact that for this IPN, the supramolecular bonds (Fe^{2+}−Tpy) are more stable than the acylhydrazone bonds and are thus dominant in the viscoelastic response. Since these bonds are quite sensitive to pH, as shown in Figure S9a for the Fe^{2+}−Tpy individual network, a significant part of these bonds dissociates at a low pH, leading to a decrease of the plateau modulus, as observed in Figure 6c. When the pH is set back to the original value, the Fe^{2+}−Tpy complexes re-form rapidly but in a less optimal configuration, yielding a network with a lower degree of cross-linking. The optimal reorganization of this "frozen" network is strongly limited due to the low lability of the Fe^{2+}−Tpy complexes.

These results show that the rheological properties of the IPN hydrogels can be finely tuned by changing the pH and that the pH sensitivity and reversibility of the gel−sol transition depends strongly on the combination of interactions used to build the IPNs.

Finally, we study the behavior of the single networks and IPNs under large deformation by performing strain sweeps (Figure 7). The three single networks (the Zn^{2+}−Tpy sample

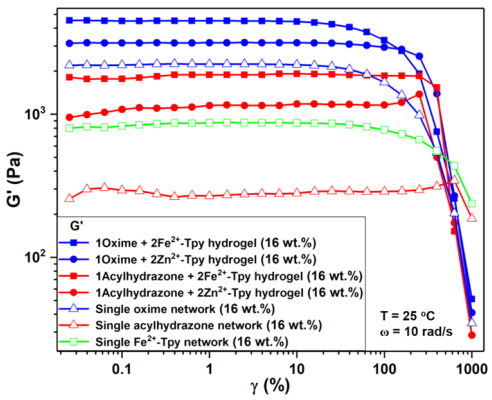

Figure 7. Oscillatory strain sweeps performed on the four IPN hydrogels and the single networks. The single Zn^{2+}−Tpy sample is not shown because it is completely relaxed under these conditions due to its fast dynamics.

https://dx.doi.org/10.1021/acs.macromol.0c00494
Macromolecules XXXX, XXX, XXX−XXX

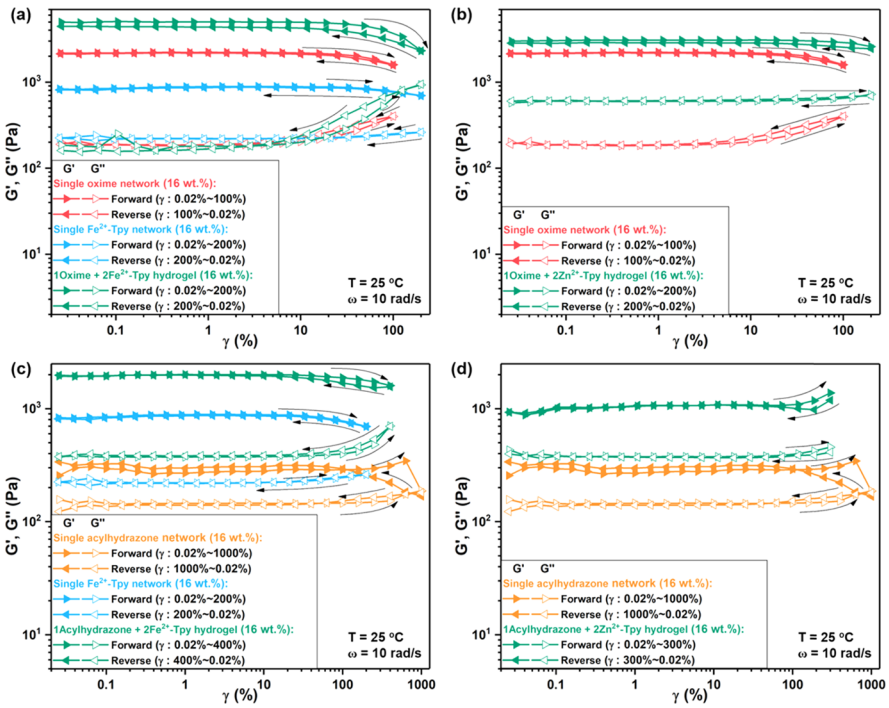

Figure 8. Oscillatory reversible strain sweeps performed on the different IPNs and their corresponding single networks: (a) 1Oxime + 2Fe^{2+}−Tpy I, (b) 1Oxime + 2Zn^{2+}−Tpy, (c) 1Acylhydrazone + 2Fe^{2+}−Tpy, and (d) 1Acylhydrazone + 2Zn^{2+}−Tpy.

is not shown since its dynamics is too fast) show a constant elastic modulus over a rather large strain range indicative of an extended linear deformation regime. The critical strain value, marking the end of the linear regime, increases in the order oxime, Fe^{2+}−Tpy, acylhydrazone, following the decrease of cross-linking density in these three networks. At large strain amplitudes, the networks cannot withstand the deformation anymore and the samples break and are expelled from the geometries. Therefore, to probe the reversibility of the bonds, measurements were performed from low strain up to the maximum strain amplitude that can be reached without destroying the sample, then from this high strain amplitude down to low strain. Under such conditions, all of the single networks fully recover their original state, as shown in Figure 8. The small hysteresis that is observed for the highly sheared samples is attributed to the strain-induced breaking of part of the reversible bonds, the latter being able to re-form when the deformation amplitude is reduced.

For the single acylhydrazone network, a slight shear thickening effect is observed at a high shear amplitude. Such behavior has already been reported in the literature for reversible networks and can be attributed to the fact that large shear flow promotes the formation of intermolecular associations.[65,66] While other mechanisms could also lead to shear thickening (such as chain stretching), an increase of intermolecular associations fits our results since when going back from high to low strain amplitude, the storage and loss moduli of this network are slightly higher than the corresponding initial values (Figure 8c,d), indicating a better organization of the network. This shear thickening property is observed only for the acylhydrazone network, which contains a large amount of nonactive cross-links and/or unreacted groups, and which did not fully reach equilibrium after an aging time of 2 days (Figure S6).

The four IPNs also show an extended linear regime. As for the single networks, as long as the strain sweep test is stopped before reaching the amplitude at which the samples break, the data measured from low to high to low strain amplitude show a good reversibility (Figure 8). Again, a hysteresis appears at a high strain. The reversible bonds are forced to break under large oscillatory shear to allow the sample to follow the deformation, but as soon as the deformation is reduced, the reversible bonds are able to quickly re-form. This shows the ability of the networks to self-heal after a large deformation.

Interestingly, the evolution of the critical strain value γ_c between the single networks and the IPNs depends on the considered combination of networks. In particular, while the stiffest IPN network, built from oxime and Fe^{2+}−Tpy bonds, has a similar γ_c value to the oxime single network, the IPN network containing oxime and the most labile supramolecular bond, Zn^{2+}−Tpy, displays a longer linear regime, corresponding to a larger γ_c value. Similarly, the linear regime of the IPN network formed from the long-lifetime Fe^{2+}−Tpy complexes and the weak acylhydrazone is longer than the linear regime of the single network formed only from the Fe^{2+}−Tpy complexes. Thus, one can conclude that using IPNs allows a significant increase of storage modulus while conserving, or even improving, the deformability of the materials.

■ CONCLUSIONS

In this work, we investigated the viscoelastic properties of interpenetrated network hydrogels based on two orthogonal types of reversible bonds: dynamic covalent bonds (DCBs) and metal−ligand bonds, with the aim of creating very stable—yet reversible—networks thanks to the presence of the DCBs, while the more tunable metal−ligand interactions can be used to adjust the material properties. In particular, we have studied how the rheological properties of both networks are combined and modified when these networks are interpenetrated. Four

https://dx.doi.org/10.1021/acs.macromol.0c00494
Macromolecules XXXX, XXX, XXX−XXX

IPN hydrogels were thus obtained by combining either a very stable and pH-insensitive DCB (oxime) or a slightly less stable and pH-sensitive DCB (acylhydrazone), with either a long-lifetime supramolecular interaction (Fe^{2+}−Tpy) or a more dynamic one (Zn^{2+}−Tpy).

The results show that the obtained IPN hydrogels exhibit a higher modulus compared to the simple addition of the moduli of the single networks. We attributed this observation to the fact that part of the entanglements between the chains of the two networks are trapped between associated stickers and, therefore, act as additional physical interactions governed by the dynamics of the stickers. The study also revealed that the partial relaxation of the IPNs is induced by the relaxation of the supramolecular network and takes place through a sticky Rouse relaxation. We then studied how lowering the pH can be used as a stimulus to affect the dynamics of the IPNs. In particular, we showed that a low pH strongly influences the stability of the acylhydrazone DCB network. At low pH, the acylhydrazone subnetwork relaxes faster than the Fe^{2+}−Tpy supramolecular network, which corresponds to an inversion of the relaxation times of the two subnetworks compared to neutral pH. Finally, we demonstrated that building IPNs allows a significant increase of storage modulus while conserving, or even improving, the deformability of the materials. Combining DCB and metal−ligand bonds seems thus a promising approach toward highly tunable interpenetrated network hydrogels. Their properties under elongation should now be investigated to study the role played by the two networks on their extensibility.

■ ASSOCIATED CONTENT

Supporting Information

The Supporting Information is available free of charge at https://pubs.acs.org/doi/10.1021/acs.macromol.0c00494.

Experimental section; synthetic routes of TPy-DEG-NH_2, TPy-DEG-AM, P(DMA-*co*-ketone), and P(DMA-*co*-Tpy); preparations of individual dynamic Schiff base bonding networks, individual metal−terpyridine bonding networks, single networks in water from mixed copolymers of P(DMA-*co*-ketone) and P(DMA-*co*-Tpy), and IPN hydrogels; ^{1}H NMR spectra of P(DMA-*co*-ketone), P(DMA-*co*-Tpy), dihydrazide, bishydroxylamine, acylhydrazone network, and oxime network; oscillatory frequency sweeps and strain sweeps; and pH dependence of the dynamic moduli (PDF)

■ AUTHOR INFORMATION

Corresponding Authors

Evelyne van Ruymbeke − *Bio and Soft Matter Division (BSMA), Institute of Condensed Matter and Nanosciences (IMCN), Université catholique de Louvain, B-1348 Louvain-la-Neuve, Belgium;* orcid.org/0000-0001-7633-0194; Email: evelyne.vanruymbeke@uclouvain.be

Charles-André Fustin − *Bio and Soft Matter Division (BSMA), Institute of Condensed Matter and Nanosciences (IMCN), Université catholique de Louvain, B-1348 Louvain-la-Neuve, Belgium;* orcid.org/0000-0002-3021-5438; Email: charles-andre.fustin@uclouvain.be

Authors

Hui Yang − *Bio and Soft Matter Division (BSMA), Institute of Condensed Matter and Nanosciences (IMCN), Université catholique de Louvain, B-1348 Louvain-la-Neuve, Belgium*

Sina Ghiassinejad − *Bio and Soft Matter Division (BSMA), Institute of Condensed Matter and Nanosciences (IMCN), Université catholique de Louvain, B-1348 Louvain-la-Neuve, Belgium*

Complete contact information is available at: https://pubs.acs.org/10.1021/acs.macromol.0c00494

Notes

The authors declare no competing financial interest.

■ ACKNOWLEDGMENTS

This project was partially funded by the French Community of Belgium through ARC project no. 16/21-076. H.Y. acknowledges the China Scholarship Council for the support of Ph.D. fellowship. E.v.R. is research associate of the FRS-FNRS.

■ REFERENCES

(1) Appel, E. A.; del Barrio, J.; Loh, X. J.; Scherman, O. A. Supramolecular Polymeric Hydrogels. *Chem. Soc. Rev.* **2012**, *41*, 6195−6214.

(2) Ulrich, S. Growing Prospects of Dynamic Covalent Chemistry in Delivery Applications. *Acc. Chem. Res.* **2019**, *52*, 510−519.

(3) Saunders, L.; Ma, P. X. Self-Healing Supramolecular Hydrogels for Tissue Engineering Applications. *Macromol. Biosci.* **2019**, *19*, No. 1800313.

(4) Heidarian, P.; Kouzani, A. Z.; Kaynak, A.; Paulino, M.; Nasri-Nasrabadi, B. Dynamic Hydrogels and Polymers as Inks for Three-Dimensional Printing. *ACS Biomater. Sci. Eng.* **2019**, *5*, 2688−2707.

(5) Li, J.; Geng, L.; Wang, G.; Chu, H.; Wei, H. Self-Healable Gels for Use in Wearable Devices. *Chem. Mater.* **2017**, *29*, 8932−8952.

(6) Shang, J.; Le, X.; Zhang, J.; Chen, T.; Theato, P. Trends in Polymeric Shape Memory Hydrogels and Hydrogel Actuators. *Polym. Chem.* **2019**, *10*, 1036−1055.

(7) Guo, Y.; Bae, J.; Zhao, F.; Yu, G. Functional Hydrogels for Next-Generation Batteries and Supercapacitors. *Trends Chem.* **2019**, *1*, 335−348.

(8) Yuk, H.; Lu, B.; Zhao, X. Hydrogel Bioelectronics. *Chem. Soc. Rev.* **2019**, *48*, 1642−1667.

(9) Voorhaar, L.; Hoogenboom, R. Supramolecular Polymer Networks: Hydrogels and Bulk Materials. *Chem. Soc. Rev.* **2016**, *45*, 4013−4031.

(10) Zou, W.; Dong, J.; Luo, Y.; Zhao, Q.; Xie, T. Dynamic Covalent Polymer Networks: from Old Chemistry to Modern Day Innovations. *Adv. Mater.* **2017**, *29*, No. 1606100.

(11) Wojtecki, R. J.; Meador, M. A.; Rowan, S. J. Using the Dynamic Bond to Access Macroscopically Responsive Structurally Dynamic Polymers. *Nat. Mater.* **2011**, *10*, 14−27.

(12) Chakma, P.; Konkolewicz, D. Dynamic Covalent Bonds in Polymeric Materials. *Angew. Chem., Int. Ed.* **2019**, *58*, 9682−9695.

(13) Liu, Y.; Lehn, J.-M.; Hirsch, A. K. H. Molecular Biodynamers: Dynamic Covalent Analogues of Biopolymers. *Acc. Chem. Res.* **2017**, *50*, 376−386.

(14) Lu, W.; Le, X.; Zhang, J.; Huang, Y.; Chen, T. Supramolecular Shape Memory Hydrogels: A New Bridge Between Stimuli-Responsive Polymers and Supramolecular Chemistry. *Chem. Soc. Rev.* **2017**, *46*, 1284−1294.

(15) Jiang, Z.-C.; Xiao, Y.-Y.; Kang, Y.; Pan, M.; Li, B.-J.; Zhang, S. Shape Memory Polymers Based on Supramolecular Interactions. *ACS Appl. Mater. Interfaces* **2017**, *9*, 20276−20293.

(16) Schäfer, S.; Kickelbick, G. Double Reversible Networks: Improvement of Self-Healing in Hybrid Materials via Combination

of Diels-Alder Cross-Linking and Hydrogen Bonds. *Macromolecules* **2018**, *51*, 6099−6110.

(17) Jiang, Z.; Bhaskaran, A.; Aitken, H. M.; Shackleford, I. C. G.; Connal, L. A. Using Synergistic Multiple Dynamic Bonds to Construct Polymers with Engineered Properties. *Macromol. Rapid Commun.* **2019**, *40*, No. 1900038.

(18) Zhang, H.; Wu, Y.; Yang, J.; Wang, D.; Yu, P.; Lai, C. T.; Shi, A.-C.; Wang, J.; Cui, S.; Xiang, J.; Zhao, N.; Xu, J. Superstretchable Dynamic Polymer Networks. *Adv. Mater.* **2019**, *31*, No. 1904029.

(19) Sheiko, S. S.; Dobrynin, A. V. Architectural Code for Rubber Elasticity: From Supersoft to Superfirm Materials. *Macromolecules* **2019**, *52*, 7531−7546.

(20) Zhang, C.; Yang, Z.; Duong, N. T.; Li, X.; Nishiyama, Y.; Wu, Q.; Zhang, R.; Sun, P. Using Dynamic Bonds to Enhance the Mechanical Performance: From Microscopic Molecular Interactions to Macroscopic Properties. *Macromolecules* **2019**, *52*, 5014−5025.

(21) Xi, W.; Scott, T. F.; Kloxin, C. J.; Bowman, C. N. Click Chemistry in Materials Science. *Adv. Funct. Mater.* **2014**, *24*, 2572−2590.

(22) Zhang, J.-Y.; Zeng, L.-H.; Feng, J. Dynamic Covalent Gels Assembled from Small Molecules: From Discrete Gelators to Dynamic Covalent Polymers. *Chin. Chem. Lett.* **2017**, *28*, 168−183.

(23) Zhang, J.; Hu, Y.; Li, Y. Dynamic Covalent Gels. *Gel Chemistry: Interactions, Structures and Properties*; Lecture Notes in Chemistry; Springer: Singapore, 2018; Vol. *96*, pp 119−151.

(24) Apostolides, D. E.; Patrickios, C. S. Dynamic Covalent Polymer Hydrogels and Organogels Crosslinked Through Acylhydrazone Bonds: Synthesis, Characterization and Applications. *Polym. Int.* **2018**, *67*, 627−649.

(25) Zhang, Z. P.; Rong, M. Z.; Zhang, M. Q. Polymer Engineering Based on Reversible Covalent Chemistry: A Promising Innovative Pathway Towards New Materials and New Functionalities. *Prog. Polym. Sci.* **2018**, *80*, 39−93.

(26) Sims, M. B.; Patel, K. Y.; Bhatta, M.; Mukherjee, S.; Sumerlin, B. S. Harnessing Imine Diversity to Tune Hyperbranched Polymer Degradation. *Macromolecules* **2018**, *51*, 356−363.

(27) Li, L.; Lin, Q.; Tang, M.; Duncan, A. J. E.; Ke, C. Advanced Polymer Designs for Direct-Ink-Write 3D Printing. *Chem. − Eur. J.* **2019**, *25*, 10768−10781.

(28) Shi, L.; Ding, P.; Wang, Y.; Zhang, Y.; Ossipov, D.; Hilborn, J. Self-Healing Polymeric Hydrogel Formed by Metal-Ligand Coordination Assembly: Design, Fabrication, and Biomedical Applications. *Macromol. Rapid Commun.* **2019**, *40*, No. 1800837.

(29) Brassinne, J.; Stevens, A. M.; Van Ruymbeke, E.; Gohy, J. F.; Fustin, C. A. Hydrogels with Dual Relaxation and Two-Step Gel-Sol Transition from Heterotelechelic Polymers. *Macromolecules* **2013**, *46*, 9134−9143.

(30) Brassinne, J.; Fustin, C. A.; Gohy, J. F. Control Over the Assembly and Rheology of Supramolecular Networks via Multi-Responsive Double Hydrophilic Copolymers. *Polym. Chem.* **2017**, *8*, 1527−1539.

(31) Winter, A.; Schubert, U. S. Synthesis and Characterization of Metallo-Supramolecular Polymers. *Chem. Soc. Rev.* **2016**, *45*, 5311−5357.

(32) Grindy, S. C.; Learsch, R.; Mozhdehi, D.; Cheng, J.; Barrett, D. G.; Guan, Z.; Messersmith, P. B.; Holten-Andersen, N. Control of Hierarchical Polymer Mechanics with Bioinspired Metal-Coordination Dynamics. *Nat. Mater.* **2015**, *14*, 1210−1216.

(33) Wu, H.; Zheng, J.; Kjøniksen, A.-L.; Wang, W.; Zhang, Y.; Ma, J. Metallogels: Availability, Applicability, and Advanceability. *Adv. Mater.* **2019**, *31*, No. 1806204.

(34) Creton, C. 50th Anniversary Perspective: Networks and Gels: Soft but Dynamic and Tough. *Macromolecules* **2017**, *50*, 8297−8316.

(35) Narita, T.; Mayumi, K.; Ducouret, G.; Hébraud, P. Viscoelastic Properties of Poly(vinyl alcohol) Hydrogels Having Permanent and Transient Cross-Links Studied by Microrheology, Classical Rheometry, and Dynamic Light Scattering. *Macromolecules* **2013**, *46*, 4174−4183.

(36) Ahmadi, M.; Seiffert, S. Thermodynamic Control over Energy Dissipation Modes in Dual-network Hydrogels Based on Metal-ligand Coordination. *Soft Matter* **2020**, *16*, 2332−2341.

(37) Liu, Y.; Tang, Z.; Wu, S.; Guo, B. Integrating Sacrificial Bonds into Dynamic Covalent Networks toward Mechanically Robust and Malleable Elastomers. *ACS Macro Lett.* **2019**, *8*, 193−199.

(38) Myung, D.; Waters, D.; Wiseman, M.; Duhamel, P.-E.; Noolandi, J.; Ta, C. N.; Frank, C. W. Progress in the Development of Interpenetrating Polymer Network Hydrogels. *Polym. Adv. Technol.* **2008**, *19*, 647−657.

(39) Dragan, E. Design and Applications of Interpenetrating Polymer Network Hydrogels. A Review. *Chem. Eng. J.* **2014**, *243*, 572−590.

(40) Klymenko, A.; Nicolai, T.; Benyahia, L.; Chassenieux, C.; Colombani, O.; Nicol, E. Multiresponsive Hydrogels Formed by Interpenetrated Self-Assembled Polymer Networks. *Macromolecules* **2014**, *47*, 8386−8393.

(41) Yu, Z.; Zhang, Y.; Gao, Z. J.; Ren, X. Y.; Gao, G. H. Enhancing Mechanical Strength of Hydrogels via IPN Structure. *J. Appl. Polym. Sci.* **2017**, *134*, No. 44503.

(42) Kausar, A. Interpenetrating Polymer Network and Nano-composite IPN of Polyurethane/ Epoxy: A Review on Fundamentals and Advancements. *Polym.−Plast. Technol. Mater.* **2019**, *58*, 691−706.

(43) Zhang, B.; Ke, J.; Vakil, J. R.; Cummings, S. C.; Digby, Z. A.; Sparks, J. L.; Ye, Z.; Zanjani, M. B.; Konkolewicz, D. Dual-Dynamic Interpenetrated Networks Tuned through Macromolecular Architecture. *Polym. Chem.* **2019**, *10*, 6290−6304.

(44) Yang, J.; Ma, M. G.; Zhang, X. M.; Xu, F. Elucidating Dynamics of Precoordinated Ionic Bridges as Sacrificial Bonds in Interpenetrating Network Hydrogels. *Macromolecules* **2016**, *49*, 4340−4348.

(45) Gong, J. P. Why Are Double Network Hydrogels So Tough? *Soft Matter* **2010**, *6*, 2583−2590.

(46) Chen, Q.; Chen, H.; Zhu, L.; Zheng, J. Engineering of Tough Double Network Hydrogels. *Macromol. Chem. Phys.* **2016**, *217*, 1022−1036.

(47) Le, X.; Lu, W.; Zheng, J.; Tong, D.; Zhao, N.; Ma, C.; Xiao, H.; Zhang, J.; Huang, Y.; Chen, T. Stretchable Supramolecular Hydrogels with Triple Shape Memory Effect. *Chem. Sci.* **2016**, *7*, 6715−6720.

(48) Xiao, H.; Lu, W.; Le, X. X.; Ma, C. X.; Li, Z. W.; Zheng, J.; Zhang, J. W.; Huang, Y. J.; Chen, T. A Multi-Responsive Hydrogel with a Triple Shape Memory Effect Based on Reversible Switches. *Chem. Commun.* **2016**, *52*, 13292−13295.

(49) Foster, E. M.; Lensmeyer, E. E.; Zhang, B.; Chakma, P.; Flum, J. A.; Via, J. J.; Sparks, J. L.; Konkolewicz, D. Effect of Polymer Network Architecture, Enhancing Soft Materials Using Orthogonal Dynamic Bonds in An Interpenetrating Network. *ACS Macro Lett.* **2017**, *6*, 495−499.

(50) Le, X.; Lu, W.; Xiao, H.; Wang, L.; Ma, C.; Zhang, J.; Huang, Y.; Chen, T. Fe^{3+}-, PH-, Thermoresponsive Supramolecular Hydrogel with Multishape Memory Effect. *ACS Appl. Mater. Interfaces* **2017**, *9*, 9038−9044.

(51) Tang, L.; Wen, L.; Xu, S.; Pi, P.; Wen, X. Ca^{2+}, Redox, and Thermoresponsive Supramolecular Hydrogel with Programmed Quadruple Shape Memory Effect. *Chem. Commun.* **2018**, *54*, 8084−8087.

(52) Zhang, F.; Xiong, L.; Ai, Y.; Liang, Z.; Liang, Q. Stretchable Multiresponsive Hydrogel with Actuatable, Shape Memory, and Self-Healing Properties. *Adv. Sci.* **2018**, *5*, No. 1800450.

(53) Wang, M.; Wang, L.; Xu, Y.; Fu, L.; Yang, H. One-Pot Fabrication of Triple Shape Memory Hydrogel Based on Coordination Bond, the Dynamic Borate Ester Bonds, and Hydrogen Bond. *Soft Mater.* **2019**, *17*, 342−349.

(54) Lewis, R. W.; Malic, N.; Saito, K.; Evans, R. A.; Cameron, N. R. Ultra-High Molecular Weight Linear Coordination Polymers with Terpyridine Ligands. *Chem. Sci.* **2019**, *10*, 6174−6183.

(55) Dirksen, A.; Dawson, P. E. Rapid Oxime and Hydrazone Ligations with Aromatic Aldehydes for Biomolecular Labeling. *Bioconjugate Chem.* **2008**, *19*, 2543−2548.

https://dx.doi.org/10.1021/acs.macromol.0c00494
Macromolecules XXXX, XXX, XXX−XXX

(56) McKinnon, D. D.; Domaille, D. W.; Cha, J. N.; Anseth, K. S. Biophysically Defined and Cytocompatible Covalently Adaptable Networks as Viscoelastic 3D Cell Culture Systems. *Adv. Mater.* **2014**, *26*, 865−872.
(57) McKinnon, D. D.; Domaille, D. W.; Cha, J. N.; Anseth, K. S. Bis-Aliphatic Hydrazone-Linked Hydrogels Form Most Rapidly at Physiological pH: Identifying the Origin of Hydrogel Properties with Small Molecule Kinetic Studies. *Chem. Mater.* **2014**, *26*, 2382−2387.
(58) Kölmel, D. K.; Kool, E. T. Oximes and Hydrazones in Bioconjugation: Mechanism and Catalysis. *Chem. Rev.* **2017**, *117*, 10358−10376.
(59) Chen, Q.; Tudryn, G. J.; Colby, R. H. Ionomer Dynamics and The Sticky Rouse Model. *J. Rheol.* **2013**, *57*, 1441−1462.
(60) Zhang, Z.; Chen, Q.; Colby, R. H. Dynamics of Associative Polymers. *Soft Matter* **2018**, *14*, 2961−2977.
(61) Ahmadi, M.; Hawke, L. G. D.; Goldansaz, H.; van Ruymbeke, E. Dynamics of Entangled Linear Supramolecular Chains with Sticky Side Groups: Influence of Hindered Fluctuations. *Macromolecules* **2015**, *48*, 7300−7310.
(62) Hawke, L. G. D.; Ahmadi, M.; Goldansaz, H.; van Ruymbeke, E. Viscoelastic Properties of Linear Associating Poly(N-butyl acrylate) Chains. *J. Rheol.* **2016**, *60*, 297−310.
(63) Brassinne, J.; Gohy, J. F.; Fustin, C. A. Orthogonal Control of the Dynamics of Supramolecular Gels from Heterotelechelic Associating Polymers. *ACS Macro Lett.* **2016**, *5*, 1364−1368.
(64) Kalia, J.; Raines, R. T. Hydrolytic Stability of Hydrazones and Oximes. *Angew. Chem., Int. Ed.* **2008**, *47*, 7523−7526.
(65) Xu, D.; Hawk, J. L.; Loveless, D. M.; Jeon, S. L.; Craig, S. L. Mechanism of Shear Thickening in Reversibly Cross-Linked Supramolecular Polymer Networks. *Macromolecules* **2010**, *43*, 3556−3565.
(66) Shangguan, Y.; Liu, M.; Luo, G.; Zheng, Q. Shear Induced Self-thickening of Chitosan/β-cyclodextrin Compound Solution. *RSC Adv.* **2016**, *6*, 110367−110374.

https://dx.doi.org/10.1021/acs.macromol.0c00494
Macromolecules XXXX, XXX, XXX−XXX